Synthesis of Indium Nanoparticles: Digestive Ripening under Mild Conditions

Sreeram Cingarapu,[†] Zhiqiang Yang,[‡] Christopher M. Sorensen,[§] and Kenneth J. Klabunde*,[†]

[†]Department of Chemistry and [§]Department of Physics, Kansas State University, Manhattan, Kansas 66506, United States
[‡]Department of Chemistry, Clemson University, Clemson, South Carolina 29634, United States

Ⓢ *Supporting Information*

ABSTRACT: Here we report the synthesis of monodispersed indium nanoparticles by evaporation/condensation of indium shot using the solvated metal atom dispersion (SMAD) technique, followed by digestive ripening in low boiling point (BP 38 °C) methylene chloride and in a high boiling point (BP 110 °C) toluene solvent. The as-prepared SMAD indium nanoparticles are polydispersed with particle size ranging from 25 to 50 nm, but upon digestive ripening (heating of colloidal material at the boiling point of solvent in presence of excess surface active ligands) in methylene chloride, a remarkable reduction of particle size was achieved. In higher boiling solvent (toluene), where the indium nanoparticles at reflux temperature are probably melted, it does not allow the best result, and less monodispersity is achieved. We employed different surface active ligands (amine, phosphine, and mixed ligands) to passivate these indium nanoparticles. The temporal evolution of the surface plasmon of indium nanoparticles was monitored by in situ UV—vis spectroscopy, and particles were characterized by transmission electron microscopy (TEM) and X-ray diffraction (XRD). The merits of this synthesis procedure are the use of bulk indium as starting material, tuning the particle size in low boiling point solvent, particle size adjustment with the choice of ligand, and a possible scale up.
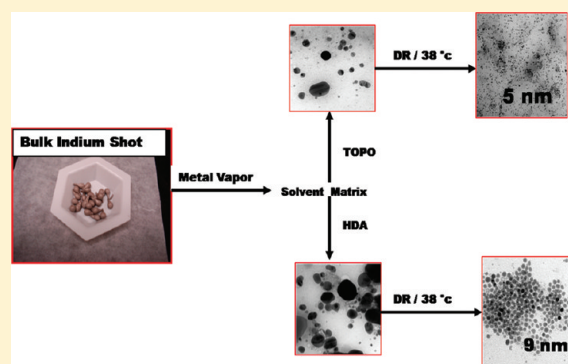
■ INTRODUCTION

In recent years, metal nanoparticles have received significant attention because of their unique properties such as melting point, conductivity, magnetism, specific heat, surface plasmon resonance (SPR), and color.[1] These nanoparticles are used in diverse fields including catalysis,[2] magnetic recording media,[3,4] microelectronics,[5,6] sensing, clinical diagnostics, surface-enhanced Raman scattering (SERS), and energy conversion.[7,8] Hence, synthesizing metal nanoparticles with narrow size distribution, uniform shape, and good crystalline nature represents a significant challenge. There are many reports and reviews on the synthesis of noble and transition metal nanoparticles, but much less work has been done on indium nanoparticle synthesis. Indium is widely used in the field of electronics including single electron transistor,[9] in nanoelectro-mechanical resonators,[10] electronic switches,[11] as a component in low melting solders,[12] solid-state lubricants,[13] detection of DNA and protein,[14—16] and as printing nanoparticle building blocks in nanoxerography.[17] Silica-encapsulated indium nanoparticles were used as a phase-change material for enhancing heat capacity[18] and as a growth promoter for the III—V semiconductor rods.[19—21] Indium acts as a catalyst in various organic reactions as well.[22—25]

In general, indium nanoparticles have been synthesized by physical and chemical methods. Physical methods involve dispersion of molten metal in paraffin oil,[26] ultrasound irradiation,[13]

laser ablation,[27] thermal evaporation followed by aerosol formation,[28] emulsification by top-down and bottom-up approaches,[29,30] sputter deposition technique in ionic liquids,[16] and oleylamine driven phase transfer synthesis.[31] Unfortunately some of these methods offer little control over particle size.[13,26] Chemical methods involve reduction of metal salts by strong reducing agents like sodium metal,[32] sodium borohydride in ionic liquids,[33] zinc powder,[26,34] alkalides and electrides,[35] and decomposition of organometallic complexes.[19,36—38] More recently, it has been reported that the morphology of indium nanoparticles can be kinetically controlled by borohydride reduction at room temperature.[39] There are a few other reports on controlling the morphology of indium nanoparticles, which involves synthesis of hollow spheres and nanotubes,[40,41] nanowires,[42] highly faced polyhedra[43] and protein cavities as the reaction chamber for the fabrication.[44] In general, to control the particle size and size distribution, a variety of protecting agents have been investigated, which includes thiols,[45] phosphines,[46] amines,[47] alkanecyanides,[48] and thioethers.[49]

This paper describes synthesis of indium nanoparticles by the metal evaporation/condensation solvated metal atom dispersion "SMAD" technique. We have found that digestive ripening[50,51]

can be used to achieve monodispersity under very mild conditions. Indeed, digestive ripening or "nanomachining" is a post preparative process that is thermodynamically controlled, and involves heating of polydispersed colloidal particles at the boiling point of the solvent in the presence of excess surface active ligands.[45,47,50−55] Choice of solvent, boiling point, and ligand is specific for each case. In some cases, even room temperature digestive ripening can be achieved.[56]

■ EXPERIMENTAL SECTION

Chemicals. Indium shot (99.9%, Strem Chemicals Inc.), hexadecylamine (HDA) (98%), trioctylphosphine oxide (TOPO) (Reagent Plus 99%), and trioctylphosphine (TOP) were purchased from Sigma-Aldrich and used without further purification. Toluene, methylene chloride, acetone, and methanol (Fisher Scientific) were used for the synthesis of nanoparticles. Toluene, acetone, and methylene chloride solvents were distilled and degassed four times by the standard freeze-thaw procedure prior to use.

Preparation Procedures. Typically, indium shot (0.3 g) was placed in a C9 boron nitride crucible (R.D. Mathis # C9-BN) resting in a metal basket (R. D. Mathis # B8B # x.030 w), which was in turn connected to water cooled copper electrodes and then the SMAD reaction chamber was charged with ligand (we chose 1:30 metal to ligand ratio based on previous work[51]) and vacuum sealed. After complete evacuation, a liquid N_2 Dewar was placed around the sealed SMAD reactor, and the ligands at the bottom of the reactor freeze because of the external liquid N_2. A schematic assembly of the SMAD reactor is shown elsewhere.[57] Once the vacuum reached 4×10^{-3} Torr, 50 mL of distilled and degassed either acetone or methylene chloride solvent was evaporated through the solvent shower head. The evaporated solvent was condensed on the wall of the SMAD reactor by external liquid N_2 cooling, which formed a uniform solvent matrix. Then the metal was heated gradually using water cooled electrodes. The vaporized metal was co-condensed with the continuous flow of co-condensing solvent vapor, and this co-condensing restricts vaporized atoms from aggregation. The temperature required for the metal vaporization is ∼900 °C, and it took nearly 2−3 h based on the amount of starting material and a total of 100−125 mL of solvent. During the heating process, heat transfer from the hot crucible to the walls of the SMAD reactor was minimized by sealing the crucible and the basket with a fibrous alumina ceramic insulator (Zircar product, Inc.) [*Caution! Note about safety and cleanliness; before starting this procedure, the SMAD reactor was cleaned with aqua regia, base bath, acid bath, and finally with copious amount of water, followed by drying. Special personal protection is necessary while working with a vacuum line, which includes eye protection. Also acids and bases used for cleaning can cause severe burns, so proper acid proof gloves and clothing protection is necessary*]. Once all the metal was vaporized, the liquid N_2 Dewar was removed. The solvent matrix along with the condensed metal appeared black in color and the matrix was allowed to melt and warm to room temperature, and the molten matrix along with the co-condensed metal slowly reaches the bottom of the SMAD reactor and mixes with the ligand. A homogeneous single phase as-prepared colloid was obtained after vigorous stirring for 30 min with a magnetic stirrer. Later, the as-prepared colloid was siphoned into a Schlenk glass tube under the protection of argon. This as-prepared SMAD product was then subjected to digestive ripening under the protection of argon.

Sample Prepared in Two-Solvent System. In two-solvent system, acetone was used as a co-condensing solvent for condensing the evaporated indium metal and toluene as a digestive ripening solvent. After siphoning indium-ligand-acetone-toluene SMAD product into a Schlenk glass tube; acetone was removed under dynamic vacuum leaving

Scheme 1. Reaction Sequence during SMAD Synthesis and Digestive Ripening of Indium Particles
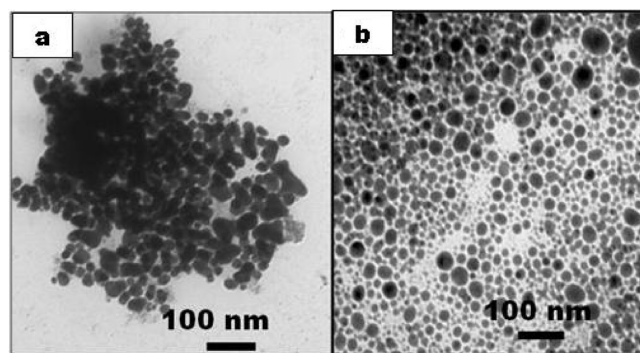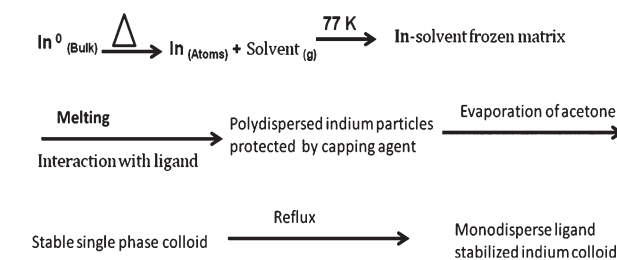

Figure 1. TEM images of trioctylphosphine coated indium nanoparticles (A) before digestive ripening and (B) after digestive ripening in toluene.
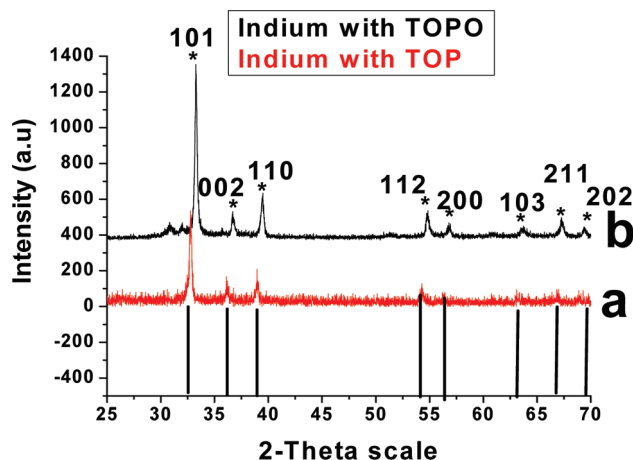

Figure 2. XRD of indium nanoparticles after digestive ripening in toluene (a) stabilized with trioctyl phosphine and (b) with trioctylphosphine oxide.

indium-ligand-toluene colloid, which was then digestively ripened in toluene at 110 °C.

Samples Prepared in Single Solvent System. In this system, methylene chloride was used as a single solvent, which served as co-condensing solvent as well as digestive ripening solvent, and digestive ripening was carried out at the boiling point (38 °C) of the solvent.

Digestive Ripening. Two solvents were used to determine the influence of the solvent boiling point on the indium nanoparticles, and three colloids were produced by carrying out digestive ripening in toluene (BP, 110 °C) and methylene chloride (BP, 38 °C). In all experiments the metal to ligand ratio is 1:30, and a heating mantle was

used for reflux. The reaction sequence during the SMAD and digestive ripening is shown in Scheme 1.

Characterization. Analyses of the particles were carried out before and after the digestive ripening. UV—vis absorption spectra were recorded using an in situ UV—vis optical fiber, assisted by a DH-2000 UV—vis optical spectrophotometer instrument (Ocean Optics Inc.). The powder X-ray diffraction (PXRD) samples were prepared by the evaporation of solvent from the indium/toluene or indium/methylene chloride dispersion loaded on XRD glass plates and PXRD patterns were recorded by a Bruker D8 X-ray diffractometer with Cu Kα radiation. The samples were scanned from $20 < 2\theta < 70°$ at an increment of 0.2°/min, and the total acquisition time period was more than 2 h. A drop of washed and redispersed colloid was suspended on a transmission electron microscopy (TEM) carbon coated grid and allowed to dry under vacuum. TEM and electron diffraction (ED) were performed on a Philips CM100 operating at 100 kV. The yields were calculated based on a previously reported method for gold-dodecanethiol SMAD digestive ripening system,[51] and were 80 ± 5% .

■ RESULTS AND DISCUSSION

Digestive ripening conditions (solvent, ligand, temperature, time) can be adjusted for each substance. For indium, we have investigated different solvents and ligands, and we have found substantial differences, which are reported below.
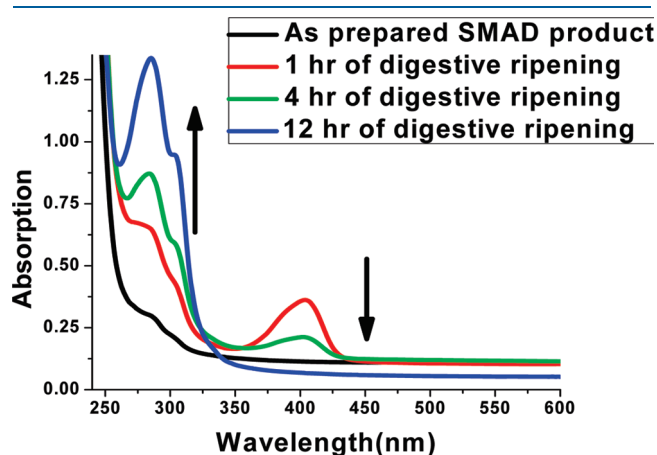
Figure 3. Temporal evolution of surface plasmon absorbance resonance peak for trioctylphosphine oxide protected indium nanoparticles. The black line represents the as-prepared SMAD colloid, and the red line represents sample after 1 h of digestive ripening, green line after 4 h, and blue line represents the surface plasmon of indium after 12 h of digestive ripening in methylene chloride.

Digestive Ripening in Toluene. The as-prepared SMAD colloid produced with trioctyl phosphine stabilized particles appeared black in color, but upon digestive ripening in toluene, the color of the sample was slightly changed from black to light brown. Addition of ethanol caused precipitation, and this precipitate was easily redissolved in toluene or chloroform. The UV—vis absorption spectrum of the as-prepared SMAD product was broad, and after digestive ripening for 1 h in toluene the peak was narrowed considerably (Supporting Information, Figure 1). As shown in Figure 1, aggregates of indium nanoparticles were broken up, but considerable polydispersity still remained. The XRD data in Figure 2 shows all the characteristic peaks of indium, and it matches with the literature data.[26]

The as-prepared SMAD indium nanoparticles protected with trioctylphosphine oxide ligands also exhibited a broad UV—vis absorption peak that narrowed somewhat after 1 h in refluxing toluene (Supporting Information, Figure 1). In toluene the ligand stabilized particles were easily dissolved and manipulated, but the digestive ripening step was only marginally successful, because, at reflux temperature, indium nanoparticles are probably molten, allowing ease of coalescence.

Digestive Ripening in Methylene Chloride. In general, in the SMAD technique two solvents were employed where one solvent was used for solvation of vaporized particles and another solvent for digestive ripening. However, it was found that methylene chloride worked well for both purposes. Figure 3 shows the UV—vis absorption spectrum of indium nanoparticles
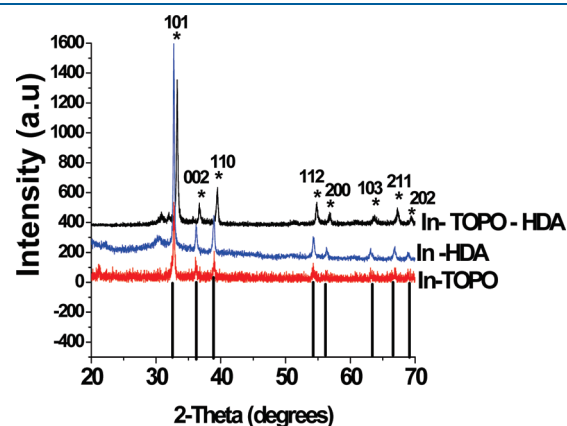
Figure 5. XRD patterns of all three indium colloids exhibit prominent peaks at scattering angles (2Θ) of 32.96, 36.31, 39.17, 54.48, 56.58, 63.21, 67.04, and 69.10, which are assigned to scattering from the 101, 002, 110, 112, 200, 103, 211, and 202 crystal planes, and all these peaks can be indexed to the body-centered tetragonal phase of indium.
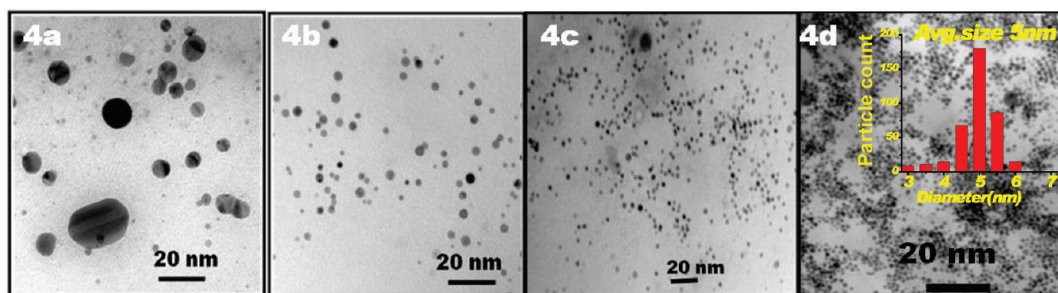
Figure 4. TEM image of (a) as-prepared polydispersed SMAD product of trioctylphosphine oxide stabilized particles, (b) after 1 h of digestive ripening, (c) after 12 h of digestive ripening, and (d) after 24 h of digestive ripening in methylene chloride solvent.

stabilized by TOPO. The as-prepared SMAD particles exhibit a little hump around 280 nm in the absorption spectrum, but during digestive ripening a new peak appeared around 400 nm, and this peak gradually vanished, but the peak at 280 nm was stabilized (indicated with arrows in Figure 3). The appearance of the new peak around 400 nm might be due to either dissolving or breaking down of bigger particles in the initial digestive ripening time, or it could be that these bigger particles have no quantum effect as suggested by one of the reviewers. Indeed, digestive ripening causes bigger particles to break down into very small particles, and these smaller particles tend to grow and finally the
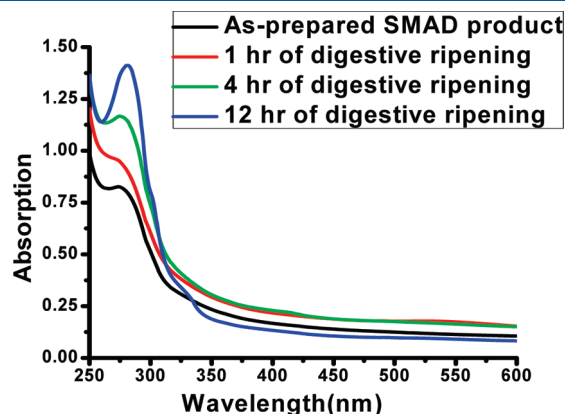

Figure 6. Temporal evolution of surface plasmon absorbance resonance peaks for hexadecylamine protected indium nanoparticles. The black line represents the as-prepared SMAD colloid, and the red line represents sample after 1 h of digestive ripening, green line after 4 h, and blue line represents the surface plasmon of indium after 12 h of digestive ripening in methylene chloride.

system reaches to an equilibrium size regime. Further, the absorption phenomenon in indium nanoparticles because of SPR is found to be both solvent and morphology dependent, and hence its absorption shifts in-between 240 and 370 nm.[26,32,33,39,40]

This narrow stable absorption peak after 24 h of digestive ripening indicates that the particles attained an equilibrium size distribution. The temporal evolution of particles is shown in Figure 4a−d. The estimated particle sizes deduced from the TEM are in the range of ∼5 nm ±0.6 nm (inset Figure 4d), where 300 particles on a selected area were manually measured. After 12 h of digestive ripening, no more change in average particle size and a small change in the UV−vis absorption intensity were observed.

The XRD patterns (Figure 5) of all three indium colloids (TOPO, HDA, and TOPO/HDA stabilized indium nanoparticles) after digestive ripening exhibit prominent peaks that can be indexed to the body-centered tetragonal indium phase. These XRD peaks were verified from the XRD data file (**SS-NNN 85−1409**) and match with the published literature.[40]

The UV−vis absorption spectrum of as-prepared hexadecyl amine stabilized indium particles is broad but upon digestive ripening the UV−vis peak becomes much sharper (Figure 6) at 290 nm wavelength.

The particles attained an equilibrium size within 24 h of digestive ripening but upon prolonged (36 h), the particle become more spherical (Figure 7a−e), and the particle mean size measured on the TEM images lies in the range of ∼9 nm ±0.5 nm, and the histogram of particles after 36 h of digestive ripening is shown in Figure 7f; the electron diffraction rings in Figure 7e correspond to lattice distance of 0.27 nm, 0.25 nm, and 0.23 nm can be indexed as rings of indium 101, 002, and 110.

Compared to neat ligands (either TOPO or HDA), the mixed ligand system has a strong UV−vis absorption peak even before
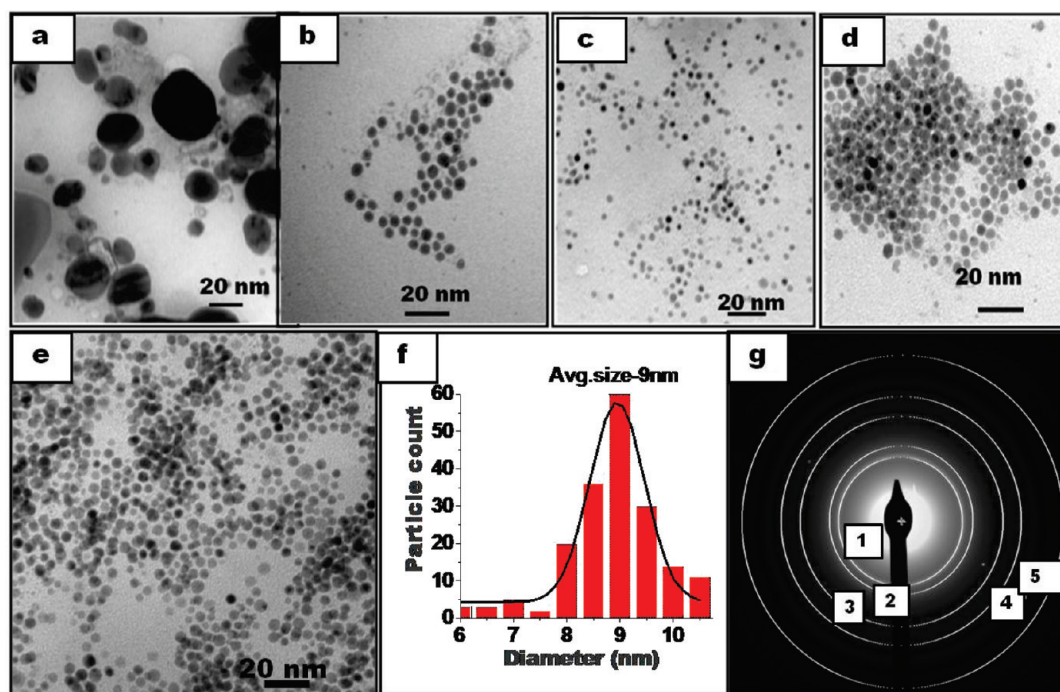

Figure 7. TEM image of (a) as -prepared polydispersed indium nanoparticles stabilized with hexadecylamine ligand, (b) after 1 h of digestive ripening, (c) after 12 h of digestive ripening, and (d) after 24 h of digestive ripening in methylene chloride; (e) after 36 h of digestive ripening, (f) particle size distribution and (g) electron diffraction patterns .
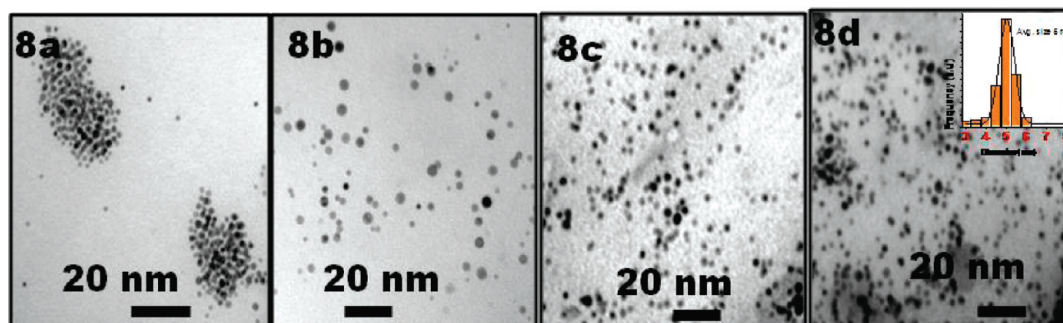
Figure 8. TEM image of (a) as -prepared polydispersed indium nanoparticles stabilized with trioctylphosphine oxide and hexadecyl amine ligand, (b) after 1 h of digestive ripening, (c) after 2 h of digestive ripening, and (d) after 4 h of digestive ripening in methylene chloride.

digestive ripening, but after digestive ripening the peak further strengthens and stabilizes at 280 nm. Further comparison of as-prepared SMAD particles with TOPO or HDA stabilized particles shows that the mixed ligand particles are relatively more soluble, and quasi-monodispersed size distribution was achieved at relatively shorter time (4 to 6 h). Figure 8a−d shows the TEM images of particles with the progress of digestive ripening. The mean size measured from TEM is ∼5 nm ± 0.5 nm. This indicates that the mixed ligand system works best for the digestive ripening of indium nanoparticles, and the XRD shows all the characteristic features of indium as seen in Figure 5. The overall ligand/solvent interaction on the UV−vis absorption, particle size, and size distribution are shown in Supporting Information, Table 1.

■ CONTROL EXPERIMENT

Surprised by these ligand effects at this low temperature, a control experiment was carried out to understand the effect of ligands on bulk metal. In this control experiment all reaction parameters were kept constant (metal to ligand (TOPO) ratio, amount of solvent (methylene chloride), and digestive ripening time, and the process was carried out under the protection of argon but with bulk indium pieces. After 3 days of digestive ripening there was no evidence of nanoparticles formation. So, this suggests that the metal vaporization is necessary, and this vaporization under dynamic vacuum leads to the formation of small crystallites or aggregates of small crystallites, and that these small particles are much more reactive than bulk indium.

■ CONCLUSIONS

Synthesis of indium nanoparticles from bulk metal has been achieved, size and monodispersity adjusted by digestive ripening. Added ligands stabilize and solubilize the nanosized material. Five new features have been uncovered: (1) Digestive ripening of indium can be carried out using a very low boiling point solvent. (2) In fact, a higher boiling solvent (toluene), where the indium nanoparticles at reflux temperature are probably molten, does not allow the best result, and less monodispersity is achieved. (3) Nanoparticle size can be varied by choice of stabilizing ligand; with TOPO in methylene chloride, 5 nm, but with hexadecyla-mine (HDA) 9 nm. Obviously, ligand choice and solvent choice are important and help control this thermodynamic phenomen-on. (4) In this case of indium, mixed ligands aid the digestive ripening process. (5) This process does not work by simply exposing bulk indium pieces to digestive ripening condition.

■ ASSOCIATED CONTENT

ⓢ Supporting Information. Further details on absorption by stabilized indium and solvent/ligand interaction before and after digestive ripening are given in Figure 1 and Table 1. This material is available free of charge via the Internet at http://pubs. acs.org.

■ AUTHOR INFORMATION

Corresponding Author
*E-mail: kenjk@ksu.edu. Phone: 785-532-6829. Fax: 785-532-6666.

■ ACKNOWLEDGMENT

■ REFERENCES

(1) Sau, T. K.; Rogach, A. L.; Jackel, F.; Klar, T. A.; Feldmann, J. Adv. Mater. 2010, 22 (16), 1805–1825.
(2) Ponce, A. A.; Klabunde, K. J. J. Mol. Catal. A: Chem. 2005, 225 (1), 1–6.
(3) Majetich, S. A.; Jin, Y. Science 1999, 284 (5413), 470–473.
(4) Black, C. T.; Murray, C. B.; Sandstrom, R. L.; Sun, S. H. Science 2000, 290 (5494), 1131–1134.
(5) Simon, U.; Flesch, R.; Wiggers, H.; Schon, G.; Schmid, G. J. Mater. Chem. 1998, 8 (3), 517–518.
(6) Tang, M. L.; Reichardt, A. D.; Miyaki, N.; Stoltenberg, R. M.; Bao, Z. J. Am. Chem. Soc. 2008, 130 (19), 6064–6065.
(7) Novak, J. P.; Brousseau, L. C.; Vance, F. W.; Johnson, R. C.; Lemon, B. I.; Hupp, J. T.; Feldheim, D. L. J. Am. Chem. Soc. 2000, 122 (48), 12029–12030.
(8) Kim, J. Y.; Yoon, S. B.; Yu, J. S. Chem. Commun. 2003, 6, 790–791.
(9) Junno, T.; Magnusson, M. H.; Carlsson, S. B.; Deppert, K.; Malm, J. O.; Montelius, L.; Samuelson, L. Microelectron. Eng. 1999, 47 (1–4), 179–183.
(10) Kim, K.; Jensen, K.; Zettl, A. Nano Lett. 2009, 9 (9), 3209–3213.
(11) Gittins, D. I.; Bethell, D.; Schiffrin, D. J.; Nichols, R. J. Nature 2000, 408 (6808), 67–69.
(12) Abtew, M.; Selvaduray, G. Mater. Sci. Eng. 2000, 27, 95–96.
(13) Li, Z.; Tao, X.; Cheng, Y.; Wu, Z.; Zhang, Z.; Dang, H. Mater. Sci. Eng., A 2005, 407 (1–2), 7–10.

(14) Wang, J.; Liu, G. D.; Zhu, Q. Y. *Anal. Chem.* **2003**, *75* (22), 6218–6222.

(15) Wang, C.; Ma, L.; Chen, L.-M.; Chai, K. X.; Su, M. *Anal. Chem.* **2010**, *82* (5), 1838–1843.

(16) Suzuki, T.; Okazaki, K.-i.; Suzuki, S.; Shibayama, T.; Kuwabata, S.; Torimoto, T. *Chem. Mater.* **2010**, *22* (18), 5209–5215.

(17) Barry, C. R.; Lwin, N. Z.; Zheng, W.; Jacobs, H. O. *Appl. Phys. Lett.* **2003**, *83* (26), 5527–5529.

(18) Hong, Y.; Ding, S.; Wu, W.; Hu, J.; Voevodin, A. A.; Gschwender, L.; Snyder, E.; Chow, L.; Su, M. *ACS Appl. Mater. Interfaces* **2010**, *2* (6), 1685–1691.

(19) Nedeljković, J. M.; Mićić, O. I.; Ahrenkiel, S. P.; Miedaner, A.; Nozik, A. J. *J. Am. Chem. Soc.* **2004**, *126* (8), 2632–2639.

(20) Li, B.; Xie, Y.; Huang, J. X.; Liu, Y.; Qian, Y. T. *Ultrason. Sonochem.* **2001**, *8* (4), 331–334.

(21) Kan, S. H.; Aharoni, A.; Mokari, T.; Banin, U. *Faraday Discuss.* **2004**, *125*, 23–38.

(22) Bang, K.; Lee, K.; Park, Y. K.; Lee, P. H. *Bull. Korean Chem. Soc.* **2002**, *23* (9), 1272–1276.

(23) Takai, K.; Ikawa, Y. *Org. Lett.* **2002**, *4* (10), 1727–1729.

(24) Lee, K.; Kim, H.; Miura, T.; Kiyota, K.; Kusama, H.; Kim, S.; Iwasawa, N.; Lee, P. H. *J. Am. Chem. Soc.* **2003**, *125* (32), 9682–9688.

(25) Schneider, U.; Ueno, M.; Kobayashi, S. *J. Am. Chem. Soc.* **2008**, *130* (42), 13824–13825.

(26) Zhao, Y.; Zhang, Z.; Dang, H.; Novel, A. *J. Phys. Chem. B* **2003**, *107* (31), 7574–7576.

(27) Ganeev, R. A.; Ryasnyanskiy, A. I.; Chakravarty, U.; Naik, P. A.; Srivastava, H.; Tiwari, M. K.; Gupta, P. D. *Appl. Phys. B: Lasers Opt.* **2007**, *86* (2), 337–341.

(28) Balamurugan, B.; Kruis, F. E.; Shivaprasad, S. M.; Dmitrieva, O.; Zahres, H. *Appl. Phys. Lett.* **2005**, *86*, 083102.

(29) Wang, Y.; Xia, Y. *Nano Lett.* **2004**, *4* (10), 2047–2050.

(30) Han, Z. H.; Cao, F. Y.; Yang, B. *Appl. Phys. Lett.* **2008**, *92*, 24.

(31) Hammarberg, E.; Feldmann, C. *Chem. Mater.* **2009**, *21* (5), 771–774.

(32) Khanna, P. K.; Jun, K.-W.; Hong, K. B.; Baeg, J.-O.; Chikate, R. C.; Das, B. K. *Mater. Lett.* **2005**, *59* (8−9), 1032–1036.

(33) Singh, P.; Kumar, S.; Katyal, A.; Kalra, R.; Chandra, R. *Mater. Lett.* **2008**, *62* (25), 4164–4166.

(34) Wang, J.; Yang, Q.; Zhang, Z. *Cryst. Growth Des.* **2009**, *9* (7), 3036–3043.

(35) Tsai, K. L.; Dye, J. L. *J. Am. Chem. Soc.* **1991**, *113* (5), 1650–1652.

(36) Soulantica, K.; Maisonnat, A.; Fromen, M.-C.; Casanove, M.-J.; Lecante, P.; Chaudret, B. *Angew. Chem., Int. Ed.* **2001**, *40* (2), 448–451.

(37) Yu, H.; Gibbons, P. C.; Kelton, K. F.; Buhro, W. E. *J. Am. Chem. Soc.* **2001**, *123* (37), 9198–9199.

(38) Soulantica, K.; Erades, L.; Sauvan, M.; Senocq, F.; Maisonnat, A.; Chaudret, B. *Adv. Funct. Mater.* **2003**, *13* (7), 553–557.

(39) Chou, N. H.; Ke, X.; Schiffer, P.; Schaak, R. E. *J. Am. Chem. Soc.* **2008**, *130* (26), 8140–8141.

(40) Zhang, Y.; Li, G.; Zhang, L. *Inorg. Chem. Commun.* **2004**, *7* (3), 344–346.

(41) Kar, S.; Santra, S.; Chaudhuri, S. *Cryst. Growth Des.* **2008**, *8* (1), 344–346.

(42) Soulantica, K.; Maisonnat, A.; Senocq, F.; Fromen, M. C.; Casanove, M. J.; Chaudret, B. *Angew. Chem., Int. Ed.* **2001**, *40* (16), 2984–2986.

(43) Lim, T. H.; Ingham, B.; Kamarudin, K. H.; Etchegoin, P. G.; Tilley, R. D. *Cryst. Growth Des.* **2010**, *10* (9), 3854–3858.

(44) Okuda, M.; Kobayashi, Y.; Suzuki, K.; Sonoda, K.; Kondoh, T.; Wagawa, A.; Kondo, A.; Yoshimura, H. *Nano Lett.* **2005**, *5* (5), 991–993.

(45) Prasad, B. L. V.; Stoeva, S. I.; Sorensen, C. M.; Klabunde, K. J. *Langmuir* **2002**, *18* (20), 7515–7520.

(46) Son, S. U.; Jang, Y.; Yoon, K. Y.; Kang, E.; Hyeon, T. *Nano Lett.* **2004**, *4* (6), 1147–1151.

(47) Prasad, B. L. V.; Stoeva, S. I.; Sorensen, C. M.; Klabunde, K. J. *Chem. Mater.* **2003**, *15* (4), 935–942.

(48) Horinouchi, S.; Yamanoi, Y.; Yonezawa, T.; Mouri, T.; Nishihara, H. *Langmuir* **2006**, *22* (4), 1880–1884.

(49) Ganesan, M.; Freemantle, R. G.; Obare, S. O. *Chem. Mater.* **2007**, *19* (14), 3464–3471.

(50) Lin, X. M.; Sorensen, C. M.; Klabunde, K. J. *J. Nanopart. Res.* **2000**, *2* (2), 157–164.

(51) Stoeva, S.; Klabunde, K. J.; Sorensen, C. M.; Dragieva, I. *J. Am. Chem. Soc.* **2002**, *124* (10), 2305–2311.

(52) Cingarapu, S.; Yang, Z.; Sorensen, C. M.; Klabunde, K. J. *Chem. Mater.* **2009**, *21* (7), 1248–1252.

(53) Heroux, D.; Ponce, A.; Cingarapu, S.; Klabunde, K. J. *Adv. Funct. Mater.* **2007**, *17* (17), 3562–3568.

(54) Smetana, A. B.; Klabunde, K. J.; Sorensen, C. M. *J. Colloid Interface Sci.* **2005**, *284* (2), 521–526.

(55) Stoeva, S. I.; Smetana, A. B.; Sorensen, C. M.; Klabunde, K. J. *J. Colloid Interface Sci.* **2007**, *309* (1), 94–98.

(56) Kalidindi, S. B.; Jagirdar, B. R. *Inorg. Chem.* **2009**, *48* (10), 4524–4529.

(57) Smetana, A. B.; Klabunde, K. J.; Marchin, G. R.; Sorensen, C. M. *Langmuir* **2008**, *24* (14), 7457–7464.

5005

dx.doi.org/10.1021/ic200232b |*Inorg. Chem.* 2011, 50, 5000–5005